On the physics of moisture-induced cracking in metal-glass (copper-silica) interfaces

J. C. Card
Department of Materials Science Engineering, University of California, Berkeley, California 94720, USA

R. M. Cannon,[a] E. Saiz, and A. P. Tomsia
Materials Sciences Division, Lawrence Berkeley National Laboratory, Berkeley, California 94720, USA

R. O. Ritchie[b]
Materials Sciences Division, Lawrence Berkeley National Laboratory, Berkeley, California 94720 and Department of Materials Science Engineering, University of California, Berkeley, California 94720, USA

(Received 16 May 2007; accepted 12 July 2007; published online 14 September 2007)

Environmentally dependent subcritical crack growth, or stress-corrosion cracking, along ceramic-metal interfaces is studied for the silica glass-copper system. Tests were conducted in various gaseous and liquid environments in order to determine their relative effects on stress-corrosion cracking and to gain some insight into the mechanisms that control interfacial crack growth. In agreement with previous studies, interfacial crack-growth rates were found to vary by orders of magnitude depending on the moisture content in gaseous environments. Water and several organic liquids, namely *n*-butanol, methanol, and N-methylformamide, were also found to promote stress-corrosion cracking. Specifically, crack-growth behavior was found to be largely dependent on the molecular structure of the test environment. Crack growth at high velocities was limited by either transport of the reactive species to the crack tip or by viscous drag contributions. Results are discussed in the context of the current mechanistic models proposed for the stress corrosion of bulk silica. © *2007 American Institute of Physics*. [DOI: 10.1063/1.2775998]

I. INTRODUCTION

The joining of two or more heterogeneous materials is essential to the successful design of components for a wide variety of applications for advanced technologies. Ceramic-metal bonding is used for structural applications such as high-temperature aerospace structures, composite materials, biomaterials, wear and corrosion resistant coated components, and electronic applications such as in the fabrication of microelectronic devices, electronic interconnections, and optical devices. These components all have mechanical properties that critically depend on the ceramic-metal interfaces contained within them.[1–4] Understanding the mechanical properties of ceramic-metal interfaces, particularly their resistance to fracture (e.g., Refs. 5–16), is vital to predicting the performance and reliability of numerous components for advanced technologies.

The integrity of such bimaterial interfaces is often characterized in terms of their resistance to fracture, as defined by a critical fracture energy G_c,[12] or fracture toughness K_c.[7] This characterization, however, may not be sufficient since components often fail at stresses far below those required for such catastrophic failure. Accordingly, it is necessary to consider, additionally, subcritical crack growth[17] and cyclically induced fracture[18] at or near these interfaces when predicting service life.

Copper/silica bonds can be processed under controlled conditions at relatively low temperature. For this reason, the Cu/SiO_2 system is an excellent model to study the basics of adhesion and fracture in non-reactive metal/ceramic interfaces. In addition, copper/glass and copper/silica interfaces play a critical role in technologies as diverse as microelectronics[19] or the development of supported Cu catalysis for the synthesis of methanol.[20] Although glass-copper interfaces have been reported to exhibit environmentally assisted subcritical crack growth at rates that vary by orders of magnitude depending on the water content of the gaseous environment in which they are tested,[17,18,21–28] complete characterization or mechanistic studies of such stress-corrosion behavior have not as yet been performed. It is the purpose of this study to examine the mechanisms that control such crack growth in the presence of water, alcohols, and other polar, reactive organic fluids. Results are discussed in the context of atomistic models of fracture and current models for the stress corrosion of bulk glass, with the objective of gaining insight into the micro-mechanisms that govern stress-corrosion crack growth along ceramic-metal interfaces.

II. BACKGROUND

A. Stress-corrosion cracking of copper

Both pure copper[29,30] and a wide range of its alloys, such as copper-zinc (brasses), or copper containing small additions of phosphorous, arsenic, antimony, silicon, nickel, or aluminum,[31] exhibit stress-corrosion cracking in a variety of environments. Susceptibility is found in moist environments

[a]Deceased.
[b]Electronic mail: roritchie@lbl.gov

 © 2007 American Institute of Physics

Downloaded 14 Sep 2007 to 131.243.15.171. Redistribution subject to AIP license or copyright, see http://jap.aip.org/jap/copyright.jsp

containing species such as ammonia, amines, nitrogen oxides, or mercury compounds. The most widely accepted mechanisms for stress-corrosion cracking of copper and its alloys are based on active-path mechanisms, which involve extremely localized dissolution processes in which specific regions are preferentially corroded. Therefore, ordinarily only environments that cause general corrosion will lead to stress-corrosion cracking under these conditions.[30,32] The environments used for the present study on glass-copper interfaces, namely air, water, methanol, *n*-butanol, and N-methylformamide, all have been found to be inactive stress-corrosion agents for both copper and its alloys[2] since these environments do not lead to appreciable active dissolution (either general or localized corrosion). Therefore, the stress-corrosion cracking of copper is unlikely to be a factor governing the stress-corrosion behavior of glass-copper interfaces.

B. Mechanisms for stress corrosion of bulk glass

Stress corrosion (or static fatigue) is an environmentally dependent mode of subcritical crack growth seen in many glasses and ceramics.[33] Crack velocity versus stress-intensity factor (v-K) plots display trimodal curves, which can be classified into three distinct regions of crack-growth behavior, as shown in Fig. 1(a). Specific studies have also indicated a threshold stress intensity below which crack growth appears dormant.[33–35]

Region I: In Region I, the crack velocity is highly dependent on the applied stress intensity and is thought to be controlled by the rate of a stress-dependent chemical reaction occurring virtually at the crack tip [e.g., Fig. 1(c)]. This chemical reaction was first described using reaction-rate theory[36–38] in which the rate of the reaction was exponentially related to an activation energy or activation barrier. Early perceptions were that the processes taking place involved the competition between crack sharpening as the crack extends and blunting due to dissolution. These processes, however, can alternatively be thought of in terms of bond rupture mechanisms.

The reaction rate for a general chemical reaction of the form $A+B \rightarrow (A-B)^{\dagger} \rightarrow C$ is given by

$$\text{rate} = (kT/h)[A][B]\exp\left(\frac{-\Delta F^{\dagger}}{RT}\right), \tag{1}$$

where k is Boltzmann's constant, T is the absolute temperature, h is Planck's constant, $[A]$ and $[B]$ are the concentrations of the reactants, R is the universal gas constant, and $\Delta F^{\dagger}$ is the change in free energy (activation barrier) of the reaction as the reaction goes to the activated state. The change in free energy, or free energy of activation, can be expressed in terms of an activation entropy $\Delta S^{\dagger}$, an activation energy $\Delta E^{\dagger}$, and an activation volume $\Delta V^{\dagger}$ as follows:

$$\Delta F^{\dagger} = -T\Delta S^{\dagger} + \Delta E^{\dagger} + P\Delta V^{\dagger}. \tag{2}$$

The above equation can be modified to describe the specific case of a chemical reaction taking place at the crack tip of a solid containing a crack. Taking into account the changes in chemical potential of the reactants and the activated complex

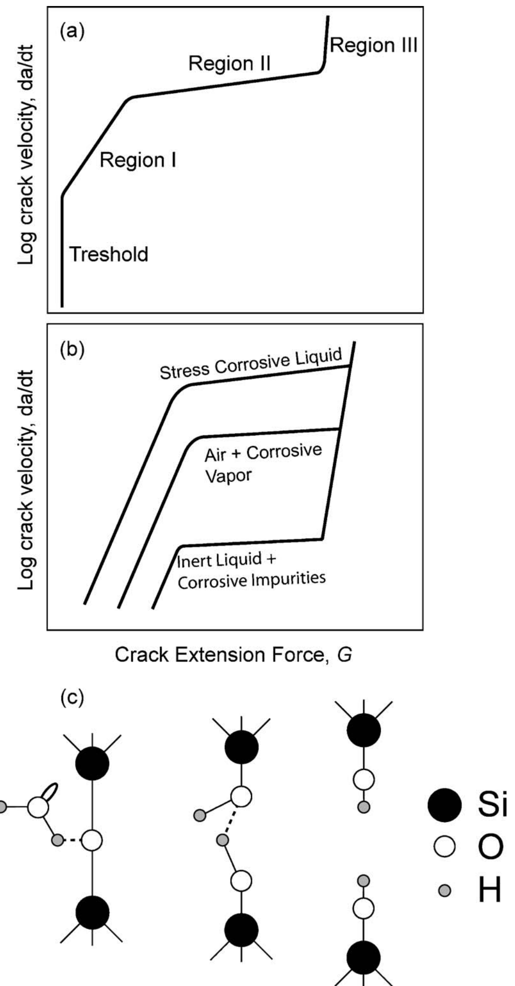

FIG. 1. Schematic illustrations of v-G curves for stress-corrosion cracking (a) along glass/copper interfaces, (b) in bulk silicate glass, and (c) associated three-step mechanism (Ref. 44) for the stress-dependent dissociative chemical reaction that occurs at the crack tip during stress corrosion in glass.

due to crack-tip curvature and crack-tip stress, the following equation is obtained for the free energy of activation:[39]

$$\Delta F^{\dagger} = -T\Delta S^{\dagger} + \Delta E^{\dagger} - \left(\frac{2K_I}{(\pi\rho)^{1/2}}\right)\Delta V^{\dagger} - (\gamma^{\dagger}V^{\dagger} - \gamma V)/\rho, \tag{3}$$

where K_I is the applied stress intensity factor, ρ is the crack-tip curvature, γ is the surface free energy of the solid, $\gamma^{\dagger}$ is the activation surface free energy, V is the partial molar volume of the material undergoing reaction, and $V^{\dagger}$ is the activation volume for the reaction. This barrier can be reduced by altering the stress state of the reactants present at the crack tip where the chemical reaction takes place. If the activation volume above is positive (which is generally the case for unimolecular bond rupture[39,40]), then the reaction will be accelerated by the application of a load to a solid containing a crack.

The activation energy can be divided into two different contributions: a stress-dependent component (mechanical energy contribution) and a stress-independent part (chemical energy contribution). Equating the rate of the chemical reaction with crack velocity, v, leads to the following relation:[37,41]

Downloaded 14 Sep 2007 to 131.243.15.171. Redistribution subject to AIP license or copyright, see http://jap.aip.org/jap/copyright.jsp

$$v = v_0 e^{(-\Delta E+\alpha K)/RT}, \quad (4)$$

where v_0 is approximately proportional to the activity of reactive species, ΔE is the stress-free activation energy, and α is a constant related to the activation volume. The above equation has been used successfully to fit Region I data for tests conducted on bulk glass. It must be pointed out that if interfacial diffusion of the active specie in the adhesive zone just behind the crack tip is the rate-controlling process, a similar dependence of the crack velocity with the applied stress could be obtained. In this case, ΔE and α in Eq. (4) will refer to diffusion barriers, rather than to adsorption ones.[42]

Region II: In Region II, crack growth is limited by the rate of transport of water, or other reactive species, to the crack tip.[43,44] In a gaseous environment, the transport is limited by the rate of diffusion of the reacting species through a stagnant region that extends a distance d behind the crack tip. The crack velocity in this plateau region is given by[43,45]

$$v_{\text{plateau}} = \frac{bDC_o}{\delta}, \quad (5)$$

where b is a constant dependent on bond length and number of bonds broken per unit area of fracture surface, C_o is the bulk concentration of the diffusing species, and D is the diffusivity of the diffusing species, which may be inversely proportional to η, the viscosity of the solution. Similar behavior obtains for specimens immersed in inert liquids in which impurities of an active species control crack extension, e.g., for toluene containing trace amounts of H_2O or for butyl alcohol containing varying amounts of water.[45]

Tests conducted on glass in liquid water also display a plateau region at high crack velocities; this case cannot be described by diffusion limitations but instead derives from viscous drag effects.[41] As the crack extends and the crack surfaces are pulled further apart, a negative pressure develops in the liquid immediately behind the crack tip (liquid is assumed to extend completely to the crack tip, i.e., complete wetting of crack surfaces). The negative pressure causes closing tractions on the crack flanks, thereby opposing the applied stress intensity. Calculations suggest that the crack-tip stress intensity, K_t, is reduced from the far-field value by the amount[45,46]

$$\Delta K = -8.76 v\eta \left(\frac{E'}{2K_t}\right)^2 (\pi a)^{1/2}, \quad (6)$$

where a is the crack length. The dependence in terms of G can alternatively be seen by using the approximation for a homogeneous material: $K=(GE')^{1/2}$. For plane-strain conditions, $E'=E/(1-\nu^2)$, where E is Young's modulus and ν is Poisson's ratio. This equation predicts a laying over or flattening of the v-G curve at higher crack growth velocities, which may be less sharp than the transition observed between Region I and the plateau region.[45,46]

Cavitation has been found to cause an abrupt transition from the plateau region into Region III for bulk glass tested in water.[47] Apparently, there is a critical crack velocity at which the pressure gradient created is not sufficient to drive the fluid fast enough to keep up with the rapidly moving crack tip. Once cavitation bubbles nucleate, they rapidly spread and largely eliminate the viscous drag. A simple model for the critical velocity at which cavitation first occurs is[47]

$$v_{\text{cav}} = \frac{(2\gamma/r) + p}{2\eta\phi^{-2}(X_2^{-1} - X_1^{-1})}, \quad (7)$$

where γ is the surface tension of the liquid, r' is the radius of the cavitation bubble, ϕ is the half-angle crack opening, p is the atmospheric pressure, and X_2 and X_1 represent the positions of the center of the cavitation bubble and the open end of the crack, respectively.

Region III: Crack growth in Region III is dictated by thermally activated processes in which inherent barriers associated with bond rupture at the crack tip must be overcome for brittle ceramics. Although crack growth seems relatively independent of environment, weak environmental dependencies have been studied for bulk glass and have been attributed to electrostatic interactions of the test environment with bonds at the crack tip.[45]

Reactive species: Studies conducted on bulk glass in various nonaqueous liquid environments[33] have shown that species other than water promote stress-corrosion crack growth provided that they have a similar molecular structure as water (a labile proton, or Bronsted acid, on one side of the molecule and a lone nonbonding electron pair, or Lewis base, on the other side, separated by a distance close to that of the Si-O bond distance of 0.163 nm); equally important, these species must reach the crack tip free of steric hindrances. Figure 1(b) shows the difference in crack-growth behavior between a liquid environment that enhances stress corrosion and one where the residual impurities are responsible for any subcritical crack growth. The large differences in the position of Region II crack growth have been used to judge whether or not a specific liquid is an aggressive stress-corrosive environment for glass.

C. Bonding at ceramic-metal interfaces

The bonding of non-reactive ceramic-metal or glass-metal couples involves the formation of an intimate or true interface. This interface can be created by atomic contact either by image and van der Waals attractive forces[49,50] or by the formation of a primary chemical bond. While there has been some discussion regarding the contribution of each type of bonding to ceramic-metal joining,[50–53] the experimental evidence and theoretical analysis indicates that chemical bonding plays a critical role.[54–56]

At a given temperature, a non-reactive oxide/metal interface can be in chemical equilibrium over a range of oxygen partial pressures. By controlling the oxygen activity it is possible to form direct metal-oxide bonds without the formation intermediate reaction layers [Fig. 2(a)]. Furthermore, inside the compatibility range, the composition of the bulk phases can change and, due to adsorption, the surface and interfacial energies and, consequently, the work of adhesion can vary with oxygen activity.[57] In any case, inside the compatibility region there could be a range of oxygen partial pressures where all the interfaces are stoichiometric. Typical works of

Downloaded 14 Sep 2007 to 131.243.15.171. Redistribution subject to AIP license or copyright, see http://jap.aip.org/jap/copyright.jsp

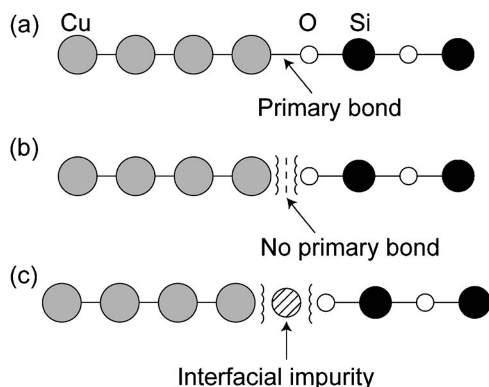

FIG. 2. Schematic illustration of bonding possibilities between a glass and a metal showing (a) primary chemical bonding, (b) van der Waals and image force bonding in which there is no electronic structure across the interface, and (c) weakening of van der Waals and image forces due to blocking and screening from interfacial impurities.

adhesion, W_{ad}, reported for stoichiometric Cu/SiO_2 interfaces vary between $\sim 0.6\ J/m^2$ for wetting experiments performed with molten copper on silica[58] to $1-4\ J/m^2$ for first-principle calculations.[17] However, impurities on the materials or in the environment can segregate to the interface, modifying the corresponding work of adhesion.[59,60] In addition, if the joining conditions (time and temperature) preclude fast diffusion and equilibration, any impurities present at bonding surfaces prior to bonding may interfere with the formation of primary bonds and limit the integrity of any subsequent secondary bonding [Fig. 2(c)]. Particularly important for the formation of strong $Cu-SiO_2$ joints is the elimination of the hydroxyl groups present on the silica surface.[17] Overall the processing conditions could result in the formation of patches of primary bonded regions surrounded by areas bonded through van der Waals and image forces as a result of impurity distributions along the interface. As an added complication the performance of the joint could be dictated to a large extent by the presence of residual interfacial pores whose shape and size are related to the contact angle and therefore to the work of adhesion.[61]

III. EXPERIMENTAL PROCEDURES

Studies were conducted using double-cantilever-beam (DCB) specimens, consisting of a 1.5 mm thick copper film bonded between two glass substrates (Fig. 3). The fused

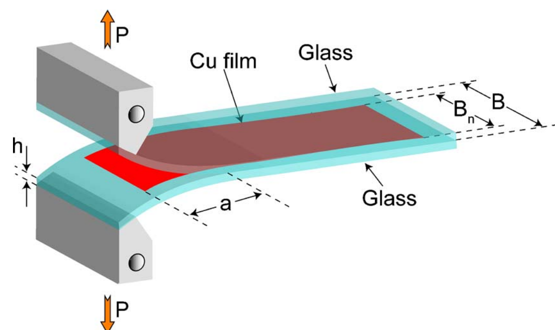

FIG. 3. (Color online) Double-cantilever-beam sandwich specimen geometry used for measurement of crack velocity versus crack extension force curves along glass-copper interfaces.

silica substrates were cleaned using a sequence of ultrasonic washes in various organic liquids: xylenes, acetone, water and Oakite™ soap, distilled water, isopropyl alcohol, triple distilled water, and a final HPLC (high-pressure liquid chromatography) grade isopropyl alcohol rinse, followed by drying at 200 °C for 2 h in room air. Samples were prepared by evaporating copper (99.99% purity) films onto each of the two fused silica substrates (of size 75 by 25 by 2 mm). A 25 mm mask was used on one substrate to provide an interfacial precrack. A 10 to 20 nm layer of chromium was evaporated onto one substrate prior to the copper in order to confine crack propagation to one interface. The substrates were then diffusion bonded at 470 °C for 2 h under a pressure of 22 MPa and a vacuum of $\sim 6 \times 10^{-4}\ N/m^2$. Under these processing conditions, interfacial fracture occurs at the Cr-free interface. To permit loading of the sample, aluminum arms were attached using epoxy.

This system has many benefits: there are no reaction layers produced during fabrication, nearly perfect planar surfaces are formed for cracks to propagate along, substrates are transparent to allow direct optical measurement of crack position, the samples are inexpensive to fabricate, stress-corrosion behavior of silica glass is well characterized, and these interfaces imitate the actual silica-metal interfaces used in industry for the production of microelectronic devices.

Moist air tests were conducted in ambient room air (~24 °C with ~40%–55% relative humidity). Testing in all other gaseous environments, specifically "dry" nitrogen and "dry" helium, was made possible by containing the specimen and loading apparatus within an environmental control chamber (~5 liter volume). For nitrogen tests, the chamber was purged with "dry" nitrogen gas (passed through Drierite™) for at least 2 h prior to testing and a constant flow rate of ~1 l/min was used to maintain a positive pressure outflow. For tests in "dry" helium, the same procedure was used except the helium was additionally passed through a liquid-nitrogen cold trap prior to entering the chamber. Testing in liquid environments, specifically water, methanol, *n*-butanol, N-methylformamide, hexane, and heptane, was achieved by immersing the bottom grip and specimen in the liquid contained in a 500 ml dish and surrounding the whole loading apparatus with an environmental control chamber. The liquids used were either anhydrous or dried over a type 4a molecular sieve for at least 1 week before use to minimize the dissolved water content. The chamber was purged with dry nitrogen gas for at least 2 h prior to the addition of each test liquid. A constant flow of ~1 l/min providing a positive pressure outflow of dry nitrogen was used to minimize the water absorbed by the liquids from the surrounding environment during testing.

Tests were conducted in triple distilled liquid water at various temperatures. Samples were first loaded in ambient air to establish the Region I crack-growth behavior; they were then tested at 3 °C by maintaining ice in the test dish, at 24 °C, which was ambient room temperature, and at 45 °C by wrapping the dish with heat tape. The order in which the temperature tests were conducted was varied in order to minimize systematic errors.

Both constant displacement and constant crosshead-

Downloaded 14 Sep 2007 to 131.243.15.171. Redistribution subject to AIP license or copyright, see http://jap.aip.org/jap/copyright.jsp

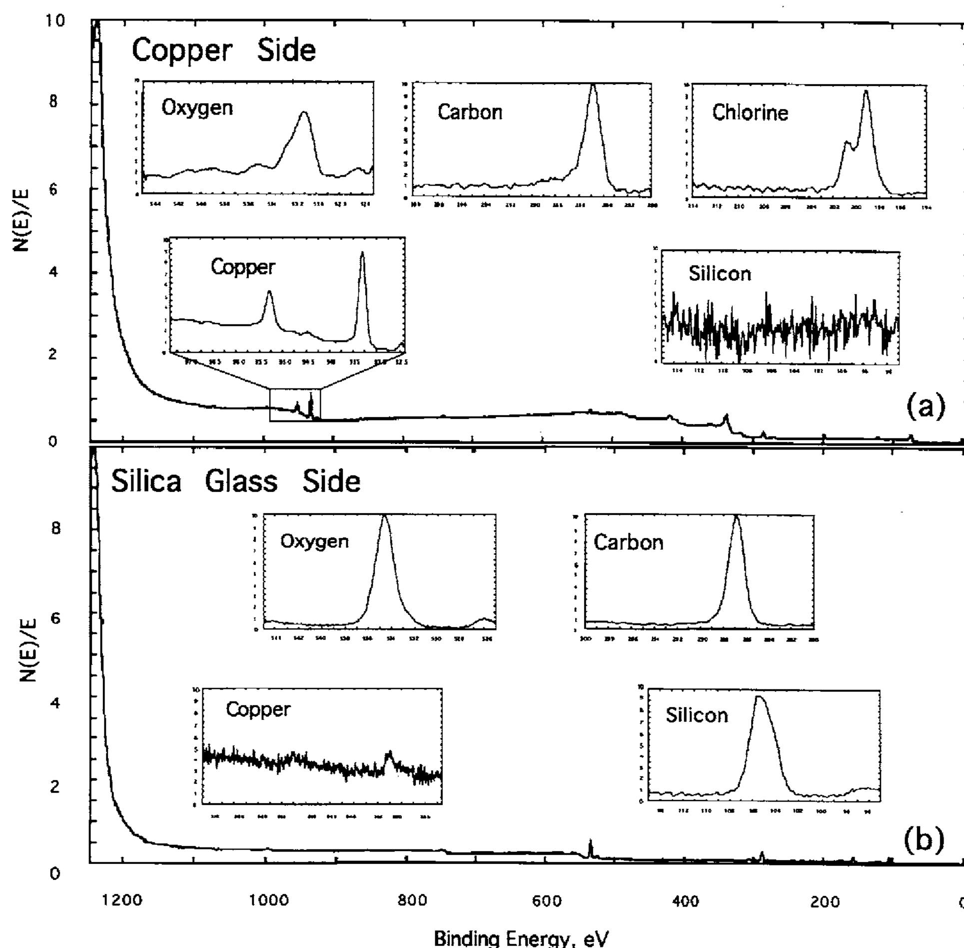

FIG. 4. Electron spectroscopy for chemical analysis (ESCA) results on the fracture of glass/Cu interface showing spectra from the (a) copper and (b) silica fracture surfaces, showing purely interfacial fracture and the presence of interfacial impurities.

speed loading conditions were used. In constant displacement tests, the samples were loaded to a predetermined value and the crosshead position was fixed. The load was then allowed to relax during crack advance. The load versus time data were converted into a crack velocity, v, versus strain energy release rate, G, plot using standard compliance relations and curve fitting. Assuming that the strain energy is largely contained within the much larger glass arms, values for G can be calculated as for a homogeneous material:[44,62]

$$G = \frac{12P^2a^2}{E'h^3BB_n}\left(1 + \frac{2h}{3a}\right)^2, \tag{8}$$

where P is the applied load, a is crack length, E' is Young's modulus in plane strain, h is the beam half height, B is the beam width, and B_n is the crack-front width. Using compliance relations for the specific case of fixed-grip geometry, the load versus time data can be converted to crack length versus time data; such data can then be incrementally curve fit using a third-order polynomial to yield crack velocities at corresponding G values.

A similar, although more complex, analysis was used for the constant crosshead-speed tests, which are more accurate for higher velocities. The constant crosshead-speed test involves loading a sample at a constant strain rate, from a load below that necessary to cause crack growth. Again, as for the fixed-grip case, the crack extension force and crack velocity can be calculated, respectively, by first converting the load versus time data into crack-length data using compliance relations. The crack-length versus time data can then be incrementally curve fit to yield crack velocities at corresponding values of G using a computer curve-fitting program.

Resulting plots of the v-G curves were consistent with those from direct optical measurements in which the transparent glass substrates and interference fringes formed permitted crack positions to be monitored using a 10× traveling microscope and a filar eyepiece; using such measurements, v-G curves were calculated using finite-difference methods.

IV. RESULTS

A. Sample variations

Due to differences in bonding and chemistry introduced during fabrication, each interface is expected to have somewhat different fracture resistance and crack-growth behavior. Electron spectroscopy for chemical analysis (ESCA) was conducted on both the copper and glass sides of the fracture surfaces of a sample fractured in liquid water [Figs. 4(a) and 4(b)]. Spectra from the copper side of the fracture surface [Fig. 4(a)] indicate the presence of carbon and chlorine impurities (presumably introduced prior to bonding during the wash procedure and exposures to air between processing steps), yet no trace of silicon. The silica side of the fracture

Downloaded 14 Sep 2007 to 131.243.15.171. Redistribution subject to AIP license or copyright, see http://jap.aip.org/jap/copyright.jsp

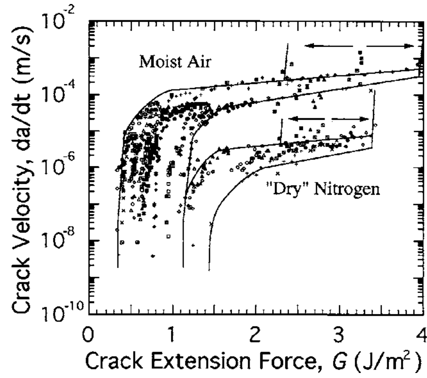

FIG. 5. Results showing two distinct scatter bands for stress-corrosion tests conducted on glass-copper interfaces in moist ambient air (~40% to 55% relative humidity) and "dry" nitrogen or helium (~0.5% relative humidity). Although there is variance in Regions I and III, Region II occurs at a relatively constant velocity for each particular humidity.

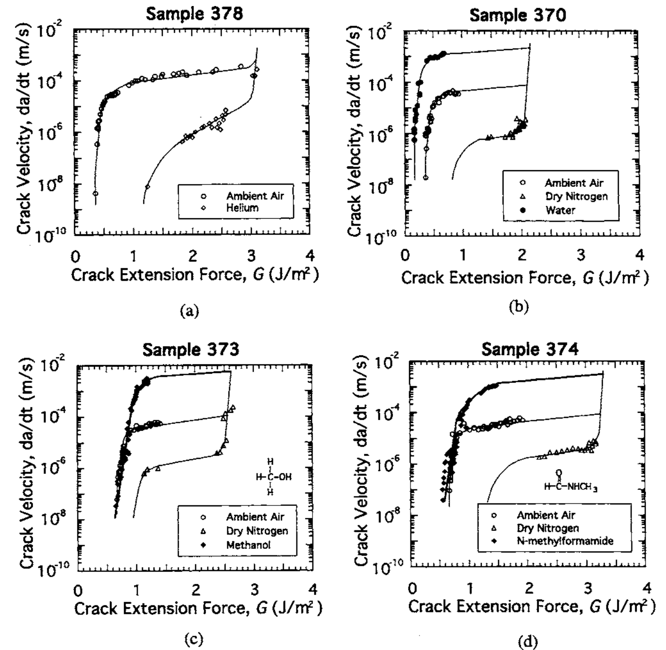

FIG. 6. Crack-growth behavior for glass/Cu interfaces conducted in ambient air and (a) dry helium, (b) dry nitrogen and liquid water, (c) dry nitrogen and methanol, and (d) dry nitrogen and N-methylformamide, showing that water, methanol and N-methylformamide are all aggressive stress-corrosion environments. The anticipated Region II for water, methanol, and N-methylformamide are a result of viscous drag contributions.

surface yields spectra [Fig. 4(b)] showing the presence of carbon impurities and minute traces of copper. These results suggest that the purely interfacial fracture that is observed is a result of interfacial impurity distributions, which may cause areas that are poorly bonded (e.g., through van der Waals and image forces) compared to other portions of the interface (dominated by primary bonding). These results are consistent with observations from *in situ* fracture studies conducted on glass-copper interfaces fabricated using nearly identical parameters.[18] Only a qualitative argument here can be given due to the difficulties in measuring the exact amount and distribution of impurities at the interface and their influence on chemistry and the bond rupture process. It is believed, however, that these impurities cause patches of poor bonding (distributed on a fine scale) amidst regions of strong primary interfacial bonding and that the overall fracture process is controlled by the rupture of these primary bonds.

Due to such chemistry differences, it is necessary to synthesize results from several samples in a way that recognizes such variations, as well as the geometry dependencies for different crack-growth regimes. Figure 5 displays the compilation of all data taken from tests conducted in gaseous environments. There are two distinct bands displayed in the figure, one enveloping the moist ambient air data and one the "dry" nitrogen or helium test data. Although there is wide scatter in Regions I and III, the Region II plateau occurs at essentially the same crack velocity for all samples tested at a particular humidity (within each band). The fact that the position of the plateau remains relatively constant from sample to sample strongly suggests that the mechanism in this region is independent of the specific sample chemistry and probably limited by transport of water to the crack tip, as is the case for stress corrosion in bulk glass.[43]

B. Tests in gaseous environments

A compilation of data for all tests conducted in moist ambient air is shown in the upper envelope of Fig. 5. There are definite differences observed in the positions of Regions I and III from sample to sample, which may be attributed to the difficulty in producing two samples that have identical chemical bonding across the interfaces. Data, taken from a sample tested in both moist ambient air and in "dry" nitrogen show a plateau for nitrogen, which occurs at a crack velocity that is orders of magnitude lower than that for ambient air [Fig. 6(d)]. This difference in the position of the plateau region is due to the variations in water vapor concentration between the two environments. At high crack velocities the curves for the two environments tend to merge in Region III and approach a common value that is independent of environment; this value, G_c, is a measure of the critical fracture energy necessary for failure without assistance from the environment.

C. Tests in liquid environments

Tests were conducted in various liquid environments, namely water, methanol, N-methylformamide, *n*-butanol, hexane, and heptane; Table I gives relevant properties of these liquids.[48,63,64] Some of these environments were used in previous studies to characterize stress-corrosion cracking in bulk glass.[46,47] Water, methanol, and N-methylformamide are all active stress-corrosion environments for bulk glass; *n*-butanol, on the other hand, possesses the necessary reactive groups but its large molecular size prohibits penetration through the small crack opening to reach the tip. Hexane and heptane, conversely, are inactive environments for stress corrosion of bulk glass because they lack the necessary polar molecular structure.

Water: Tests conducted in liquid water, moist ambient air, and "dry" nitrogen show that water accelerates crack growth with respect to ambient air [Fig. 6(b)]. The observed plateau for water occurs at a crack velocity of ~1.5–2

Downloaded 14 Sep 2007 to 131.243.15.171. Redistribution subject to AIP license or copyright, see http://jap.aip.org/jap/copyright.jsp

TABLE I. Physical properties at room temperature (25 °C) of the liquids used in this study.

Liquid	Formula	Molecular diameter (nm)	Vapor pressure (Pa)	Surface tension, γ (mJ/m^2)	Viscosity, η (mN·s/m^2)	γ/η (m/s)	Dielectric constant, ε
Water	H_2O	0.265	3.2×10^3	73.05	0.894	81.71	80.4
Hexane	C_6H_{14}		2.0×10^4	18.43	0.386	47.75	1.89
Heptane	C_7H_{16}		6.1×10^3	20.14	0.294	68.50	1.95
n-butanol	$C_4H_{10}O$	0.53	8.2×10^2	24.60	2.620	9.390	17.1
N-methylformamide	C_2H_5NO	0.45	0.3×10^2	37.96	1.678	22.62	182.4
Methanol	CH_3OH	0.359	1.7×10^4	22.61	0.547	41.33	32.6

$\times10^{-3}$ m/s. This plateau position cannot be defined by diffusion limitations [e.g., Eq. (5)], but rather by viscous drag contributions [Eqs. (6) and (7)], as described above for bulk glass.

Methanol: Methanol was found to be an aggressive environment for stress-corrosion cracking of glass-copper interfaces [Fig. 6(c)]. Behavior in methanol is similar to that of ambient air, except at higher crack velocities where methanol has a much larger accelerating effect. The measured slope of Region I for methanol yields an activation area of 0.15 nm^2, which seems to be somewhat less than that for either ambient air, 0.21 nm^2 or water, 0.20 nm^2. (The activation area, defined in Eq. (9) below, is the area corresponding to the activation volume, which is the difference in partial molar volume between the reactants and the activated complex. In the present case, the activation area is a direct function of the slope of the v-G curve in Region I [Eq. (9)].) This difference may be explained by differences in both the chemical reactions taking place at the crack tip for each environment and molecular size related limitations involved with the crack-tip region. The data indicate the onset of a plateau region at a crack velocity of $\sim4\times10^{-3}$ m/s, which again is associated with viscous drag effects.

N-methylformamide: N-methylformamide was also found to be an aggressive environment for stress-corrosion cracking of glass/Cu interfaces [Fig. 6(d)] although growth rates were only marginally faster than in ambient air, except at higher crack velocities. A distinct plateau region is seen at a crack velocity of $\sim1\times10^{-3}$ m/s. The slope of Region I for N-methylformamide gives an activation area of 0.11 nm^2, which is less than that for methanol, moist air, or water.

n -butanol: n-butanol does not result in stress corrosion of bulk glass due to steric hindrance caused by its relatively large molecular size;[37] however, in the present study, it was found to cause stress-corrosion cracking along glass-copper interfaces [Fig. 7(a)]. The accelerating effects of *n*-butanol on subcritical crack growth are smaller than in moist air at all measured crack velocities, although a very pronounced plateau region can be seen at a velocity of $\sim7-8\times10^{-4}$ m/s. The slope of the Region I curve, representing an activation area of 0.07 nm^2, is the lowest of all environments tested.

Heptane and hexane: Heptane and hexane were not found to be active stress-corrosion environments [Figs. 7(b) and 7(c)]; the acceleration in subcritical crack growth seen at low crack velocities (which is very similar to that for "dry" nitrogen) appears to result from residual water impurities dissolved in the liquid. Heptane and hexane differ from the other liquid environments tested in that they have a different molecular structure; both molecules are nonpolar whereas water, methanol, *n* -butanol, and N-methylformamide all are polar. Within experimental error, behavior in both environments approaches a common critical value of crack extension force, G_c, at high crack velocities.

D. Tests at various temperatures

Tests in water at 3, 24, and 45 °C showed Region I growth rates to be exponentially increased with temperature over the range tested; in addition, growth rates in water always exceeded those in ambient air [Fig. 7(d)]. An Arrhenius plot of these Region I data (Fig. 8) displayed a linear relationship, confirming this exponential dependence; this plot further implies that Region I is controlled by an activated

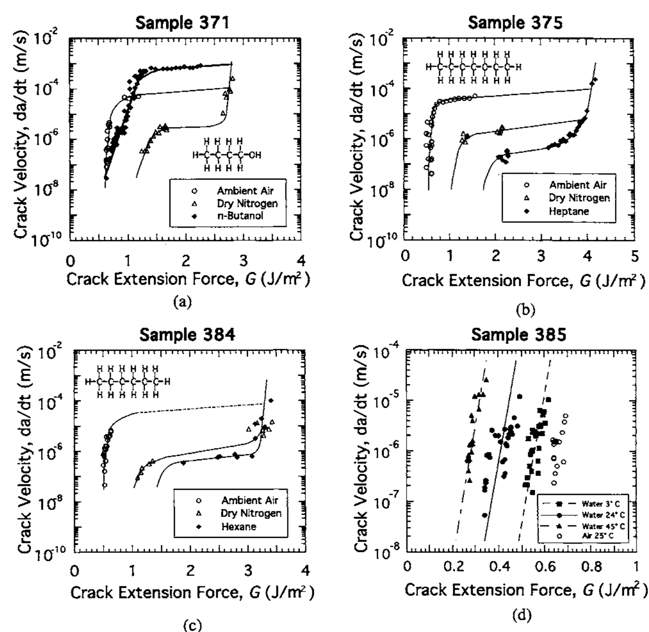

FIG. 7. Crack velocity versus crack extension plots for stress-corrosion tests conducted on glass/Cu interfaces in ambient air, dry nitrogen, and (a) *n*-butanol, (b) heptane, (c) hexane, and (d) tests in water at various temperatures. *n*-butanol accelerates crack growth relative to moist ambient air and displays a viscous drag induced plateau, while heptane and hexane are seen to be inert.

Downloaded 14 Sep 2007 to 131.243.15.171. Redistribution subject to AIP license or copyright, see http://jap.aip.org/jap/copyright.jsp

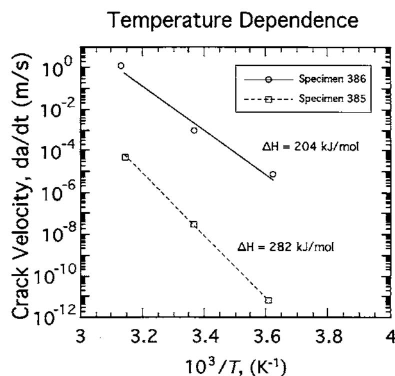

FIG. 8. Arrhenius plot for stress-corrosion tests conducted on glass/Cu interfaces in liquid water at various temperatures.

process, with an activation energy of ~204–282 kJ/mol, i.e., most likely involving a stress-dependent chemical reaction, similar to behavior in bulk glass.

V. DISCUSSION

A. Dependence on humidity

The rate of crack growth for stress-corrosion cracking along glass-copper interfaces was found to vary by orders of magnitude depending on the water content of the test environment, confirming results from previous studies.[1] Figure 6(a) shows data from a sample tested in ambient air (~50% relative humidity) and "dry" helium (~0.1% to 0.5% relative humidity). The plateau in ambient air occurs at a crack velocity of $\sim 2\times 10^{-4}$ m/s. The expression for the diffusional-induced plateau developed for bulk glass [Eq. (5)] predicts a crack velocity for the onset of the "dry" helium plateau of 4×10^{-7} to 2×10^{-6} m/s; this value corresponds closely to the actual plateau observed for the helium data [Fig. 6(a)]. This suggests that Region II for glass-copper interfaces obeys the same type of diffusion-controlled relation as that for bulk glass, i.e., the crack velocity is limited by the rate of diffusion of reactive species to the crack tip.

B. Reactive species

Water, methanol, *n*-butanol, and N-methylformamide were all found to promote stress-corrosion cracking along glass-copper interfaces, while hexane and heptane were not. Similar to behavior in bulk glass, the molecular structure of the environmental species was found to be important in determining which species will be reactive. Unlike the nonaggressive species, the aggressive species all have a similar molecular structure, i.e., a lone pair of electrons on one side of the molecule and a proton donor on the other side. Specifically, the same molecules that were reactive for bulk glass were also found to be reactive for glass-copper interfaces, with the exception of *n*-butanol (which, for the case of bulk glass, was prohibited to reach the crack tip due to its large molecular size). The similarities in the environments that are reactive for glass-copper interfaces and bulk glass suggest that the chemical reaction taking place at the crack tip may be very similar to that for bulk silica glass, i.e., the Si-O dissociative chemisorption, as described above [Fig. 1(c)].

C. Activation energy

Data for crack growth in Region I can be fit using a modified form of Eq. (4):

$$v = v_o\, e^{(-\Delta H + AG)/RT}, \qquad (9)$$

where ΔH is the activation enthalpy and A is the activation area (associated with the activation volume). An Arrhenius plot for each of the two samples tested in water between 3 and 45 °C gives values for ΔH of ~204–282 kJ/mol (Fig. 8). As these activation energies are much larger than any value reported for diffusion of water in bulk silica and silica surfaces,[65,66] this seems to rule out a diffusion-controlled process. The variance in these values is not unexpected since there are clearly differences in interfacial chemistry from sample to sample; furthermore, because the v-G curves are so steep, small changes in G will produce large changes in crack-growth rate and hence ΔH. The presence of residual porosity at the interface and the variability in the crystallographic orientation of the copper film can also contribute to the variability in the results.

As the typical bond strength of a primary bond is ~150–900 kJ/mol (Ref. 64) (e.g., the Si-O bond in bulk glass has a bond energy of ~370 kJ/mol)[67] whereas that of a secondary or van der Waals type bond is ~1–20 kJ/mol,[67] bonding across the glass-copper interfaces must involve primary chemical bonding; moreover, the activation energy for stress-corrosion cracking of such interfaces must be associated with the rupture of these primary interfacial bonds. Although impurities at the interface may act to reduce the total number of primary interfacial bonds present, thereby reducing the overall strength of the interface which may be characterized by a shift in Regions I and III, the critical bond rupture process for stress-corrosion cracking must involve the scission of the primary bonds.

D. Region I crack growth

The test environment can be seen to have a marked effect on both the slope (activation area) and driving force for Region I crack growth. For example, Fig. 5 shows a major shift in the position of the Region I curve for water compared to that for moist air. This acceleration in crack-growth behavior can be explained in the context of an atomistic model of fracture. The crack front during fracture can be modeled simply as a straight line separating severed from intact bonds, as shown in Fig. 9(a). Macroscopically, subcritical crack advance cannot occur by the simultaneous scission of all the bonds located along the crack front since the activation energy for this process is too large. Alternatively crack advance can take place by the nucleation of a localized kink[41,68] and subsequent lateral spread of these kinks along the crack front [Fig. 9(b)]. A kink site is defined as a bond that is strained enough so that its reactivity is drastically increased. Kink motion can be described as the chemical reaction of an active site with an environmental molecule to produce a ruptured bond. The rate of macroscopic crack advance can then be seen to depend on two frequency factors: (i) the rate of nucleation of active kink sites, e.g., associated with the rate of chemisorption of environmental molecules to

Downloaded 14 Sep 2007 to 131.243.15.171. Redistribution subject to AIP license or copyright, see http://jap.aip.org/jap/copyright.jsp

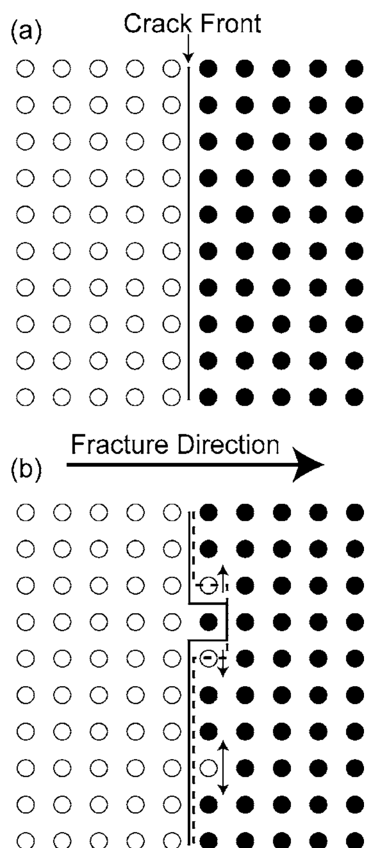

FIG. 9. Atomistic model of fracture showing (a) two-dimensional crack front modeled as a straight line separating broken (open symbols) from intact bonds (closed symbols) and (b) kinked crack front.

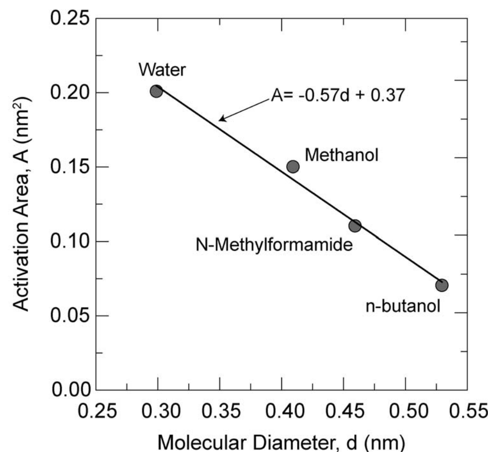

FIG. 10. Dependence of activation area on the molecular diameter of the reactive species.

strained bonds, and (ii) the rate of lateral spread of kink sites across the crack front, i.e., the rate of the bond rupture reaction. Accordingly, the acceleration in crack growth (shift in Region I), seen in moist ambient air, compared to "dry" gaseous nitrogen or helium containing only trace amounts of water (Figs. 5–7), can be explained by the increase in the number of active sites with adsorbed molecules in moist air from the larger quantity of reactive species present. A similar effect is seen for tests in water relative to those in ambient air [Figs. 6(b) and 7(d)].

The activation volume, which is directly related to the activation area, is the difference in the partial molar volume between the reactants and the activated complex; it can be affected by changes in the molecular dimensions as the reaction proceeds to the activated state. Two major factors are generally considered in estimating the activation volume: (i) structural changes that occur during the reaction, such as the degree of stretching of the bond being broken, and (ii) the formation, destruction, or alteration of charges that change the volume of the fluid surrounding the molecule through the process of electrostriction. Electrostriction models predict that the contribution to the activation volume from electrostriction processes is directly related to the dielectric constant of the test environment.[46] Table I, however, displays the dielectric constants for the liquid environments used in this study and shows that there is no relationship seen between the dielectric constants and the overall activation volumes that are a function of the Region I slopes (compare with Fig. 10). Since the electrostriction contribution is negligible compared to the contributions due to bond stretching, the activation volume for the bond rupture reaction for glass-copper interfaces can be considered to be primarily associated with the amount of bond stretching necessary to cause the dissociative reaction to occur. The larger the degree of bond straining before the formation of the activated complex, the smaller is the increase in volume after its formation (the smaller the activation volume or the activation area). Physical and chemical factors affect the degree of bond straining before rupture. The bonds should be stretched to widen the crack and allow access of the molecules to the active sites at the crack tip, and stretching the bonds also enhances their reactivity, promoting the formation of an activated complex and the subsequent bond rupture.

The measured slopes of Region I crack growth are a function of the environment, with activation areas varying between 0.21 and 0.07 nm^2. This is in contrast to bulk glass where the Region I slopes were found to be independent of the exact molecular structure (the nature of the chemical group or groups attached to the reactive group) of the stress-corrosive environment.[68] These activation areas are also larger than those reported for silicate glasses on water environments (0.01 nm^2).[42] This difference can be explained by considering the reactivity of the bonds being broken in bulk glass and in glass/Cu interfaces. The silicon oxygen bond in silica glass is relatively inert and straining of the bond at the crack tip increases its reactivity by several orders of magnitude.[68] The environmental species do not react with bonds at the crack tip at a significant rate until they are strained to a critical value. Conversely, for glass-copper interfaces, it seems that the reactive species can strongly interact with the bond being broken before it is strained enough to cause a dissociative reaction to occur; this interaction, in effect, changes the activation area (determined by the slope of Region I) necessary for the chemical reaction responsible for bond rupture.

There is an observed dependence of the activation area on the molecular size of the reactive species; the larger the molecule, the smaller the activation area (Fig. 10). This dependence can be attributed to a decrease in the effectiveness

Downloaded 14 Sep 2007 to 131.243.15.171. Redistribution subject to AIP license or copyright, see http://jap.aip.org/jap/copyright.jsp

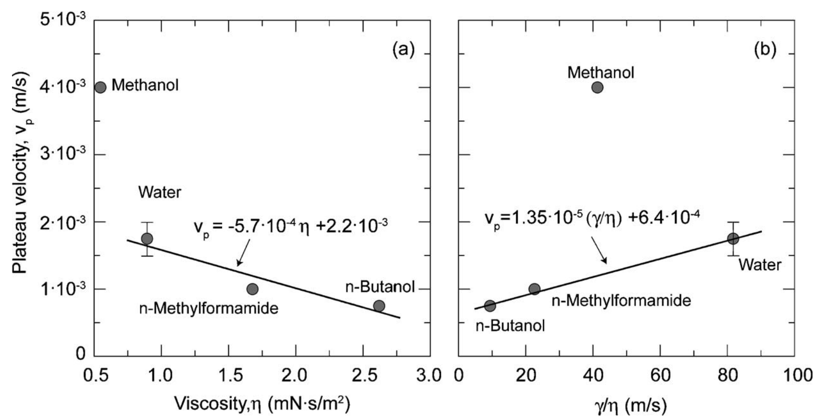

FIG. 11. Comparison of experimental plateau velocities with liquid viscosity (a) and with γ/η (b). With the exception of methanol in (b), the behavior follows expected trends.

of chemical energy contributions in overcoming the activation barrier; there is more stretching required, and hence higher G values, to pull the crack surfaces apart in order to allow large molecules to freely access the crack tip region. Using a linear fitting, a critical molecular diameter of $\sim$0.65 nm can be defined for which $A=0$. This could correspond to a molecular size for which the stretching required to allow access to the crack tip will be enough to break the bonds without a chemical contribution.

E. Viscous drag

Viscous drag contributions can play a major role in liquid environments in limiting crack-growth behavior at high crack velocities. Water, methanol, N-methylformamide, and n-butanol all display plateaus induced by the effect of such viscous drag at crack-growth velocities ranging from $\sim$0.7 to 5×10^{-3} m/s; the position of the plateau is inversely proportional to the viscosity of the test liquid (Fig. 11), as described by Eq. (6). By curve fitting the linear portion of the v-G curve (Region I) for each liquid environment, inserting the result into Eq. (6), and using the approximation for a homogeneous material, $K=(GE')^{1/2}$, the positions of the viscous drag induced plateaus can be predicted. The predicted curves, shown in Fig. 12, all correspond closely to the experimental data, except that they occur at slightly lower crack velocities. However, limited plasticity in the copper tends to open the crack-tip profile, and hence reduce the induced negative pressure in the fluid at the crack tip relative to that in a brittle homogenous material. This reduction in pressure will reduce the closing tractions along the crack flank, causing the plateau to occur at higher velocities than predicted.

The extent of the viscous drag induced plateaus is limited by cavitation effects, as discussed above for bulk glass. From Eq. (7), the critical velocity for cavitation is proportional to the ratio of surface tension to viscosity for the liquid, i.e., $v_{\text{cav}} \propto \gamma/\eta$. If cavitation were controlling the extent of Region II, the highest measured plateau velocities would be expected to scale with the ratio of γ/η (Fig. 11); however, the present data are not sufficient to support this hypothesis because of difficulties in the measurement of growth rates at very high velocities. In any case, the data suggest that methanol is the only liquid that escapes from the predicted trends. A possible explanation lies in the fact that the vapor pressure of methanol is much larger than for the other liquids (Table I). Vapor transport can facilitate the access of the reactive molecules to the crack tip, delaying the apparition of the plateau. In addition, the situation is more complex in that contact angle contributions may alter the fluid mechanics at the crack tip. While the plateau may be important for brief exposures of components to active liquids, crack-growth studies in the present study were focused at lower crack velocities because they are the prime basis of life-prediction analyses.

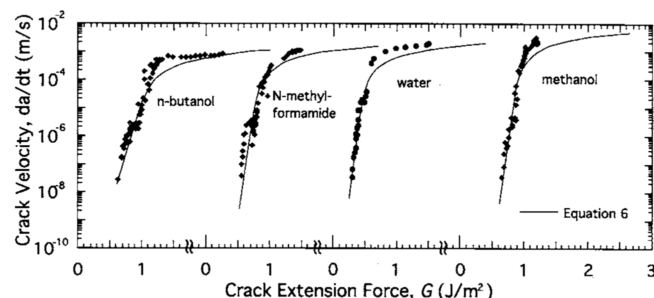

FIG. 12. Comparison of plateaus predicted from viscous drag calculations [using Eq. (6)] with experimental data for stress-corrosion tests conducted on glass/Cu interfaces in n-butanol, N-methylformamide, water, and methanol.

F. Steric hindrance

The small crack-opening displacements associated with the fracture of brittle materials may impose steric constraints and limit the access of reactive species into the crack-tip region; this may have an important influence on whether a given environment will promote stress-corrosion cracking. n-butanol, which does not cause bulk glass to stress corrode due to steric hindrances, was found to actively promote stress-corrosion cracking along glass-copper interfaces. The limited plasticity in the thin metal layer is sufficient to increase the crack-tip opening displacements, δ_0, such that larger molecules can participate in the crack-tip reaction. Figure 13 shows the crack-tip profiles for both (a) bulk glass and (b) a glass-copper interface crack at the maximum sustainable loads, i.e., G_c, and at the apparent threshold conditions, G_{TH} . The crack-tip profile for bulk glass was calculated using the plane-strain relation for the half-width of the crack opening, γ_o,[58]

Downloaded 14 Sep 2007 to 131.243.15.171. Redistribution subject to AIP license or copyright, see http://jap.aip.org/jap/copyright.jsp

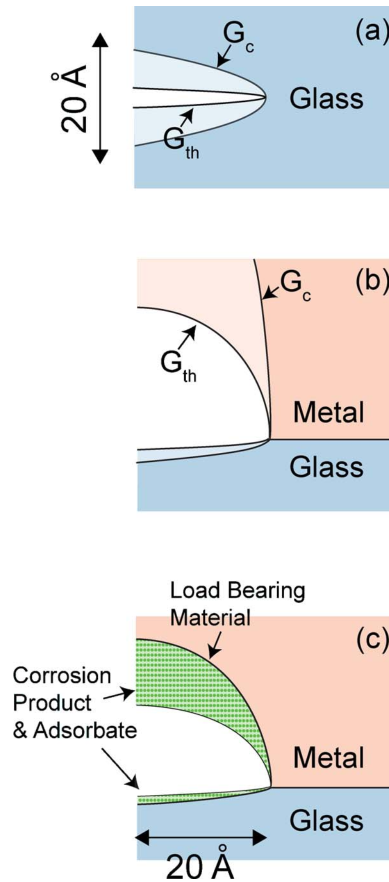

FIG. 13. (Color online) Calculated crack profiles for (a) loading at G_c, the maximum possible force, and (b) at G_{TH}, the threshold for glass (assuming purely elastic continuum behavior), and for glass-copper (assuming continuum plastic and elastic behavior in the copper and glass, respectively); (c) crack profile showing changes in effective crack-opening dimensions as a result of adsorbate and corrosion product formation.

$$y_o = \left(\frac{2K_I}{E'}\right)\left(\frac{r}{2\pi}\right)^{1/2}, \qquad (10)$$

where r is the distance back from the crack tip along the plane of the crack. The crack-tip profile for a crack along a glass-copper interface was calculated using Eq. (10) for the glass side and using blunting solutions for the copper side:[69]

$$\delta_0 = \frac{2G}{\sigma_y}, \qquad (11)$$

where σ_y is the yield stress for the copper. As shown in Fig. 13, only molecules of Ångstrom size (0.45 nm from experiment[37]) can reach the crack tip for bulk glass whereas molecules several times larger may access the crack tip for glass-copper interfaces. These profiles, however, show the dimensions of the load-bearing material and do not reflect any modifications due to adsorbate or reaction products, which may further reduce access [Fig. 13(c)].

G. Threshold region

For moist air and water environments, there is clear evidence of threshold below which crack growth becomes vanishingly small. This threshold is thought to result from adsorbate and corrosion product formation along the crack walls, which acts to block access to the crack tip. As the crack extends, reactive species react with the fresh fracture surfaces that are formed; the rate of accumulation of these corrosion products and adsorbates will be proportional to the time they are given to react. There is a balance between the rate of accumulation and the crack velocity (rate of production of fresh surfaces). At sufficiently low crack velocities, the corrosion products and adsorbates from each side of the crack mouth may impinge on one another and block access to the crack-tip region, producing the observed threshold effect. The apparent lack of a threshold for tests in other organic fluids may be a result of a lower rate of formation of adsorbates and hence a threshold that may occur at a lower crack velocity (below the measured range of velocities).

VI. CONCLUSIONS

The current study on moisture-induced stress-corrosion cracking in glass-copper interfaces provides confirmation that resulting behavior can be characterized in terms of three regimes of crack-growth: Region I, which is highly stress dependent, Region II, which is relatively stress independent, and Region III, which is essentially insensitive to the environment. Moreover, the rates of such stress-corrosion crack growth are confirmed to vary by orders of magnitude depending on the water content of the gaseous environment, with crack velocities increasing with increase in water content. Based on this work, the following new conclusions can be made:

(1) Crack growth in Region I is controlled by the rate of a stress-dependent chemical reaction involving dissociative adsorption of primary interfacial bonds at the crack tip. Akin to stress corrosion in silicate glass, the bonds which may be involved are the Si-O bonds between the glass and the oxide of the metal.
(2) Crack growth in the Region II plateau is controlled by the rate of transport of reactive species to the crack tip in inert fluid environments containing corrosive impurities and by viscous drag effects in active stress-corrosive liquid environments.
(3) Region III has been found to be essentially independent of environment as strain-energy release rates approach the fracture instability of the interface at high crack velocities. Crack growth is limited by the rate of thermally-activated processes associated with breaking primary bonds at the crack tip (without aid from the environment).
(4) An apparent threshold stress intensity was observed, below which crack growth did not occur. This threshold may be associated with blocking of the crack-tip region by formation and impingement of corrosion products and adsorbates along the crack walls.
(5) In addition to water, methanol, *n*-butanol, and N-methylformamide were found to be aggressive stress-corrosion environments. These species all have similar molecular structures, i.e., a proton donor on one side of the molecule and a lone pair of electrons on the other. Species which lack such polar molecular structure, spe-

Downloaded 14 Sep 2007 to 131.243.15.171. Redistribution subject to AIP license or copyright, see http://jap.aip.org/jap/copyright.jsp

cifically hexane and heptane, were not found to cause stress-corrosion cracking along glass-copper interfaces.

(6) The enlargement in the crack-tip profile for cracks along glass/Cu interface compared to bulk glass, due to limited plasticity in the copper, may allow much larger molecules to access the crack-tip region. Environments, such as *n*-butanol, which are inactive for the stress corrosion of glass, are thus detrimental to glass-copper interfaces.

(7) The activation area (related to the slope of the Region I crack-growth regime) was found to be inversely dependent on the molecular size of the reactive species. This dependence is thought to be caused by the decrease in effectiveness of chemical contributions in overcoming the activation barrier; specifically, the crack walls must be pulled further apart to allow larger molecules to access the crack-tip region freely.

ACKNOWLEDGMENT

This work was supported by the Director, Office of Science, Office of Basic Energy Sciences, Materials Sciences and Engineering Division of the U.S. Department of Energy under Contract No. DE-AC02-05CH11231.

[1]A. J. Blodgett, Jr., Sci. Am. **249**, 86 (1983).
[2]W. T. Chen and C. W. Nelson, IBM J. Res. Dev. **3**, 179 (1979).
[3]L. B. Freund and S. Suresh, *Thin Film Materials: Stress, Defect Formation and Surface Evolution* (Cambridge U. P., Cambridge, UK, 2003).
[4]K. K. Chawla, *Composite Materials, Science and Engineering* (Springer-Verlag, New York, 1987).
[5]G. Elssner, T. Suga, and M. Turwitt, J. Phys. **46**, 597 (1985).
[6]A. G. Evans and M. C. Lu, Acta Metall. **34**, 1643 (1986).
[7]R. M. Cannon, V. Jayaram, B. J. Dalgleish, and R. M. Fisher, in *Ceramic Microstructures '86: Role of Interfaces*, edited by J. A. Pask and A. G. Evans (Plenum, New York, 1987), p. 959.
[8]T. S. Oh, J. Rödel, R. M. Cannon, and R. O. Ritchie, Acta Metall. **36**, 2083 (1988).
[9]A. G. Evans, B. J. Dalgleish, M. He, and J. W. Hutchinson, Acta Metall. **37**, 3249 (1989).
[10]M. De Graef, B. J. Dalgleish, M. R. Turner, and A. G. Evans, Acta Metall. Mater. **40**, S333 (1992).
[11]A. G. Evans and B. J. Dalgleish, Acta Metall. Mater. **40**, S295 (1992).
[12]H. F. Wang and W. W. Gerberich, Acta Metall. Mater. **41**, 2425 (1993).
[13]R. O. Ritchie, R. M. Cannon, B. J. Dalgleish, R. H. Dauskardt, and J. M. McNaney, Mater. Sci. Eng., A **166**, 221 (1993).
[14]J. M. McNaney, R. M. Cannon, and R. O. Ritchie, Int. J. Fract. **66**, 227 (1994).
[15]F. Gaudette, S. Suresh, A. G. Evans, G. Dehm, and M. Rühle, Acta Mater. **45**, 3503 (1997).
[16]V. Imbeni, J. J. Kruzic, G. W. Marshall, S. J. Marshall, and R. O. Ritchie, Nat. Mater. **4**, 229 (2005).
[17]T. Sung Oh, R. M. Cannon, and R. O. Ritchie, J. Am. Ceram. Soc. **70**, c-352 (1987).
[18]R. M. Cannon, B. J. Dalgleish, R. H. Dauskardt, T. S. Oh, and R. O. Ritchie, Acta Metall. Mater. **39**, 2145 (1991).
[19]K. Nagao, J. B. Neaton, and N. W. Ashcroft, Phys. Rev. B **68**, 125403 (2003).
[20]L. A. Fisher and A. T. Bell, J. Catal. **178**, 153 (1998).
[21]J. M. McNaney, R. M. Cannon, and R. O. Ritchie, Acta Mater. **44**, 4713 (1996).
[22]F. Gaudette, S. Suresh, and A. G. Evans, Metall. Mater. Trans. A **30A**, 763 (1999).
[23]J. J. Kruzic, R. A. Marks, M. Yoshiya, A. M. Glaeser, R. M. Cannon, and R. O. Ritchie, J. Am. Ceram. Soc. **85**, 2531 (2002).
[24]J. J. Kruzic, J. M. McNaney, R. M. Cannon, and R. O. Ritchie, Mech. Mater. **36**, 57 (2004).
[25]M. E. Thurston and A. T. Zehnder, Acta Metall. Mater. **41**, 2985 (1993).
[26]K. Nagao, J. B. Neaton, and N. W. Ashcroft, Phys. Rev. B **68**, 125403 (2003).
[27]M. Z. Pang and S. P. Baker, J. Mater. Res. **20**, 2420 (2005).
[28]D. D. Gandhi, A. P. Singh, and M. Lane, J. Appl. Phys. **101**, 084505 (2007).
[29]K. Sieradzki and J. S. Kim, Acta Metall. Mater. **40**, 625–635 (1992).
[30]K. Sieradzki, R. L. Sabatini, and E. C. Newman, Metall. Trans. A **15A**, 1941 (1984).
[31]D. H. Thompson and A. W. Tracy, J. Met. **1**, 100 (1949).
[32]*Corrosion*, edited by L. L. Shreir (Newnes-Butterworths, Boston, 1978), Vol. 1.
[33]S. W. Freiman, J. Geophys. Res. **89**, 4072 (1984).
[34]A. G. Evans, J. Mater. Sci. **7**, 1137 (1972).
[35]T. Fett, J. P. Guin, and S. M. Wiederhorn, Eng. Fract. Mech. **72**, 2774 (2005).
[36]S. Glasstone, K. J. Laidler, and H. Eyring, *The Theory of Rate Processes; The Kinetics of Chemical Reactions, Viscosity, Diffusion and Electrochemical Phenomena* (McGraw-Hill, New York, 1941).
[37]R. J. Charles and W. B. Hillig, in *Symposium on Mechanical Strength of Glass and Ways of Improving It* (Union Scientifique Continentale du Verre, Charleroi, Belgium, 1962), p. 511.
[38]W. B. Hillig and R. J. Charles, in *High-Strength Materials*, edited by V. F. Zackey (Wiley, New York, 1965), p. 682.
[39]S. M. Wiederhorn, E. R. Fuller, Jr., and R. Thomson, Met Sci. **14**, 450 (1980).
[40]K. J. Laidler, *Chemical Kinetics* (McGraw-Hill, New York, 1965).
[41]S. M. Wiederhorn, in *Fracture Mechanics of Ceramics*, edited by R. C. Bradt, D. P. H. Hasselman, and F. F. Lange (Plenum, New York, 1978), Vol. 4, p. 549.
[42]B. R. Lawn and T. R. Wilshaw, *Fracture of Brittle Solids* (Cambridge U. P., London, UK, 1975).
[43]S. M. Wiederhorn, J. Am. Ceram. Soc. **50**, 407 (1967).
[44]S. M. Wiederhorn and L. H. Bolz, J. Am. Ceram. Soc. **53**, 543 (1970).
[45]S. M. Wiederhorn, S. W. Freiman, E. R. Fuller, and C. J. Simmons, J. Mat. Sci. **17**, 3460 (1982).
[46]T. A. Michalske and S. W. Freiman, J. Am. Ceram. Soc. **66**, 284 (1983).
[47]T. A. Michalske and V. D. Frechette, J. Am. Ceram. Soc. **63**, 603 (1980).
[48]T. A. Michalske and B. C. Bunker, J. Am. Ceram. Soc. **70**, 780 (1987).
[49]A. M. Stonham and P. W. Tasker, in *Ceramic Microstructures '86: Role of Interfaces*, edited by J. A. Pask and A. G. Evans (Plenum, New York, 1987), p. 155.
[50]D. F. Duffy, J. H. Harding, and A. M. Stoneham, Acta Metall. Mater. **40**, 511 (1992).
[51]N. Eustathopoulos and B. Drevet, Mater. Sci. Eng., A **249**, 176 (1998).
[52]D. M. Lipkin, J. N. Israelachvili, and D. R. Clarke, Philos. Mag. A **76**, 715 (1997).
[53]E. Saiz, A. P. Tomsia, and R. M. Cannon, in *Ceramic Microstructures. Control at the Atomic Level*, edited by A. P. Tomsia and A. M. Glaeser (Plenum, New York, 1998), p. 65.
[54]C. Scheu, Interface Sci. **12**, 127 (2004).
[55]C. Scheu, M. Gao, S. H. Oh, G. Dehm, S. Klein, A. P. Tomsia, and M. Ruhle, J. Math. Sci. **41**, 5161 (2006).
[56]W. Zhang, J. R. Smith, and A. G. Evans, Acta Mater. **50**, 3803 (2002).
[57]D. M. Lipkin, D. R. Clarke, and A. G. Evans, Acta Mater. **46**, 4835 (1998).
[58]R. Molins, I. Rouzou, and P. Y. Hou, Oxid. Met. **65**, 263 (2006).
[59]E. Saiz, R. M. Cannon, and A. P. Tomsia, Acta Mater. **47**, 4209 (1999).
[60]P. Shen, H. Fujii, and K. Nogi, Scr. Mater. **52**, 1259 (2005).
[61]B. J. Dalgleish, E. Saiz, A. P. Tomsia, and R. M. Cannon, and R. O. Ritchie, Scr. Metall. Mater. **31**, 1109 (1994).
[62]S. M. Wiederhorn, A. M. Shorb, and R. L. Moses, J. Appl, Physica **39**, 1569 (1968).
[63]*Handbook of Chemistry and Physics*, 72nd ed., edited by D. R. Lide (CRC, Boca Raton, FL, 1991).
[64]*Lange's Handbook of Chemistry*, 13th ed., edited by J. A. Dean (McGraw Hill, New York, 1970).
[65]P. B. McGinnis and J. E. Shelby, J. Non-Cryst. Solids **179**, 185 (1994).
[66]N. Koone, Y. Shao, and T. W. Zerda, J. Phys. Chem. **99**, 16976 (1995).
[67]J. N. Israelachvili, *Intermolecular and Surface Forces* (Academic, London, 1991).
[68]T. A. Michalske and B. C. Bunker, J. Appl. Phys. **56**, 2686 (1984).
[69]C. F. Shih, J. Mech. Phys. Solids **29**, 305 (1981).

Downloaded 14 Sep 2007 to 131.243.15.171. Redistribution subject to AIP license or copyright, see http://jap.aip.org/jap/copyright.jsp